JOURNAL OF GEOPHYSICAL RESEARCH, VOL. 105, NO. B6, PAGES 13,735–13,754, JUNE 10, 2000

Lithospheric assembly and modification of the SE Canadian Shield: Abitibi-Grenville teleseismic experiment

Stéphane Rondenay,[1] Michael G. Bostock,[1] Thomas M. Hearn, [2]
Donald J. White,[3] and Robert M. Ellis[1]

Abstract. This paper presents the results of a joint Lithoprobe-Incorporated Research Institutions for Seismology (IRIS)/Program for Array Seismic Studies of the Continental Lithosphere (PASSCAL) teleseismic experiment that investigates portions of the Grenville and Superior Provinces of the Canadian Shield along the Québec-Ontario border. Data from a 600-km-long, N-S array of 28 broadband seismographs deployed between May and October 1996 have been supplemented with additional recordings from an earlier 1994 deployment and from stations of the Canadian National Seismograph Network and the Southern Ontario Seismic Network. Relative delay times of P and S waves from 123 and 40 teleseismic events, respectively, have been inverted for velocity perturbations in the upper mantle and reveal a low-velocity, NW-SE striking corridor that crosses the southern portion of the line at latitude 46°N and lies between 50 and 300 km depth. Multievent SKS-splitting results yield an average delay time of 0.57±0.22 s and a direction of fast polarization of N93°E±18°, which is consistent with an earlier interpretation as being due to fossil strain fields related to the last major regional tectonic event. Subtle variations in splitting parameters over the low-velocity corridor may suggest an associated disruption in mantle fabric. Profiling of radial receiver functions reveals large and abrupt variations in Moho topography, specifically, a gradual thickening in crust from 40 to 45 km between latitudes 45°N and 46°N, which is followed by an abrupt thinning to 35 km at 46.6°N, some 65 km southeast of the Grenville Front. This structure is interpreted as a subduction suture extending the full length of the Front and punctuating a major pre-Grenvillian (Archean-Proterozoic) episode of lithospheric assembly in the southeast Canadian Shield. The low-velocity mantle corridor, by contrast, is better explained as the extension of the Monteregian-White Mountain-New England seamount hotspot track below the craton and is here postulated to represent interaction of the Great Meteor plume with zones of weakness within the craton developed during earlier rifting episodes.

1. Introduction

Cratons are generally associated with the idea of stability, a property which is due, at least in part, to the deep lithospheric roots that render them resistant to major structural reworking [*Jordan,* 1978; *Hoffman,* 1990]. The detailed architecture of the roots is currently a topic of great interest as it holds the clues to two important issues in solid Earth science: (1) the manner of assembly and stabilization of early continental landmasses and (2) the nature of processes which have served to modify cratonic lithosphere in its post-stabilization evolution, for example, those responsible for kimberlite volcanism or the emplacement of giant mafic dike swarms.

Over the past 2 decades, considerable progress has been made on these issues using a variety of tools. Near-surface studies (geological mapping, geochemistry, geochronology, and paleomagnetics) have supplied strong evidence that plate tectonics have been active as far back as Archean time [*Ludden and Hubert,* 1986; *Hoffman,* 1988; *De Wit et al.,* 1992; *Kimura et al.,* 1993]. Recent, high-resolution seismic experiments provide supporting documentation in the form of images of mantle reflectors merging with overlying crust in the vicinity of ancient continental sutures [*BABEL Work-*

[1]Department of Earth and Ocean Sciences, University of British Columbia, Vancouver, British Columbia, Canada.
[2]Physics Department, New Mexico State University, Las Cruces, New Mexico.
[3]Geological Survey of Canada, Ottawa, Ontario, Canada.

Paper number 2000JB900022.
0148-0227/00/2000JB900022$09.00

ing Group, 1990; *Calvert et al.,* 1995; *Warner et al.,* 1996; *Cook et al.,* 1998]. A complex mantle stratigraphy apparently persists throughout the continental lithospheric column as revealed by deeper-probing seismological investigations [*Revenaugh and Jordan,* 1991; *Bostock,* 1998].

Widespread, if infrequent, Phanerozoic kimberlite volcanism indicates that continental roots are not completely static entities but continue to evolve in the present day. Some authors [*Sykes,* 1978; *Crough et al.,* 1980] have suggested a genetic relation between kimberlites and hotspot tracks, here defined as linear, anorogenic volcanic chains mapped over oceanic and young continental lithospheres. The termination of these features over thickening continental roots has been cited as evidence supporting the origin of hotspot tracks in the interaction of fixed mantle plumes with an overriding plate [*Morgan,* 1972; *Burke and Wilson,* 1976; *Crough et al.,* 1980; *Sleep,* 1990a; *Duncan and Richards,* 1991], although compelling arguments may also be made for association of hotspot tracks with ancient rifts and subvertical lithospheric discontinuities [*Currie,* 1976; *Sykes,* 1978; *Anderson,* 1998].

This paper presents results from a teleseismic experiment conducted across the Superior and Grenville Provinces of the Canadian Shield. The results reveal lithospheric structures that are apparently related to both craton assembly during a major Precambrian compressional event and subsequent alteration associated with the Cretaceous Monteregian hotspot track. A brief tectonic overview is provided in section 2, followed by a presentation of results from analyses of body wave travel time inversion, SKS splitting and P wave receiver functions. The paper concludes with a discussion of the implications of the results for the evolution of mantle lithosphere in the southeastern Canadian Shield.

2. Tectonic Overview of the Study Area and Geophysical Coverage

The region of interest in this study is shown in Figure 1 and encompasses a variety of geological terranes with ages that range from late Archean in the northern portion of the region to Paleozoic in the south. The northern, older part comprises the Archean Superior Province of the Canadian Shield, which consists of a sequence of generally east-west trending volcano-plutonic (granite-greenstone), metasedimentary, plutonic, and high-grade gneiss subprovinces [*Card and Ciesielski,* 1986]. Formations of the Superior Province included in the study area are (from north to south) (1) the Opatica plutonic belt, which is interpreted as the deeply eroded core of an Archean orogen [*Benn et al.,* 1992; *Sawyer and Benn,* 1993]; (2) the volcano-plutonic Abitibi subprovince, a major greenstone belt [*Ludden and Hubert,* 1986]; and (3) the Pontiac metasedimentary subprovince, which is interpreted as a turbidite fan formed by the erosion of the terranes situated immediately to the north [*Kimura et al.,* 1993]. The Abitibi subprovince is truncated to the west by the Kapuskasing Structural Zone (KSZ), which represents a section of high-grade Archean lower crust thrust to the surface during the Early Proterozoic (circa 1.9 Ma [*Percival and West,* 1994]). The southern portion of the study area is within the Grenville Province, which is composed of Proterozoic and reworked Archean rocks that were strongly deformed and metamorphosed during the Grenvillian orogenic cycle (~1190-980 Ma [*Rivers,* 1997]). The Superior and Grenville Provinces are separated by the continuous SW-NE trending Grenville Front, a major crustal discontinuity that is the locus of important uplift, change in metamorphic grade, faulting, and mylonitization [*Rivers et al.,* 1989]. In the southernmost portion of the study area, Paleozoic sedimentary rocks uncomformably overlie basement rocks of the Grenville Province.

Late Jurassic to Early Cretaceous diamond-bearing kimberlites have been documented for at least two locations in the study area: the "Rapide des Quinze" kimberlites (maximum age of 126 Ma [*Ji et al.,* 1996]) and the Kirkland Lake kimberlite field (age ranging between 147 and 158 Ma [*Meyer et al.,* 1994, and references therein]). Kimberlite magmatism in the region has been associated with the same event responsible for the emplacement of the Cretaceous Monteregian-White Mountains-New England Seamounts (MWN) igneous series (see top inset in Figure 1 [*Sykes,* 1978; *Crough et al.,* 1980; *Adams and Basham,* 1991]). The trend defined by these three igneous series will be referred to here as the MWN hotspot track. These series are composed mainly of alkaline rocks showing a general age progression from west to east, with radiometric ages dating the Monteregian Hills at 124 ± 1 Ma [*Foland et al.,* 1986], the Cretaceous pulse of the White Mountains at 125-100 Ma [*Foland and Faul,* 1977], and the New England Seamounts at 103-83 Ma [*Duncan,* 1984].

The study area has been the focus of extensive geophysical investigation, as part of the Lithoprobe Abitibi-Grenville transect [*Clowes,* 1997]. Magnetotelluric surveys have revealed the presence of upper mantle electrical anisotropy [*Kellett et al.,* 1994; *Mareschal et al.,* 1995; *Sénéchal et al.,* 1996], which is believed to be related to interconnected grain boundary graphite precipitated from hydrothermal activity during major Archean tectonic events [*Mareschal et al.,* 1995]. Shear wave splitting analysis of data from a small array crossing the Grenville Front shows the existence of similar seismic anisotropy, with principal directions corresponding (within a systematic ~20° obliquity) to those of the electrical anisotropy [*Sénéchal et al.,* 1996; *Ji et al.,* 1996] and to the general orientation of major deformation zones in the area. The splitting results are thus interpreted as a "frozen-in" fabric related to the last major tectonic event to have affected the area, more than 1 Gyr ago [*Sénéchal et al.,* 1996; *Ji et al.,* 1996]. *Ji et al.* [1996] further interpret the systematic ~20° obliq-

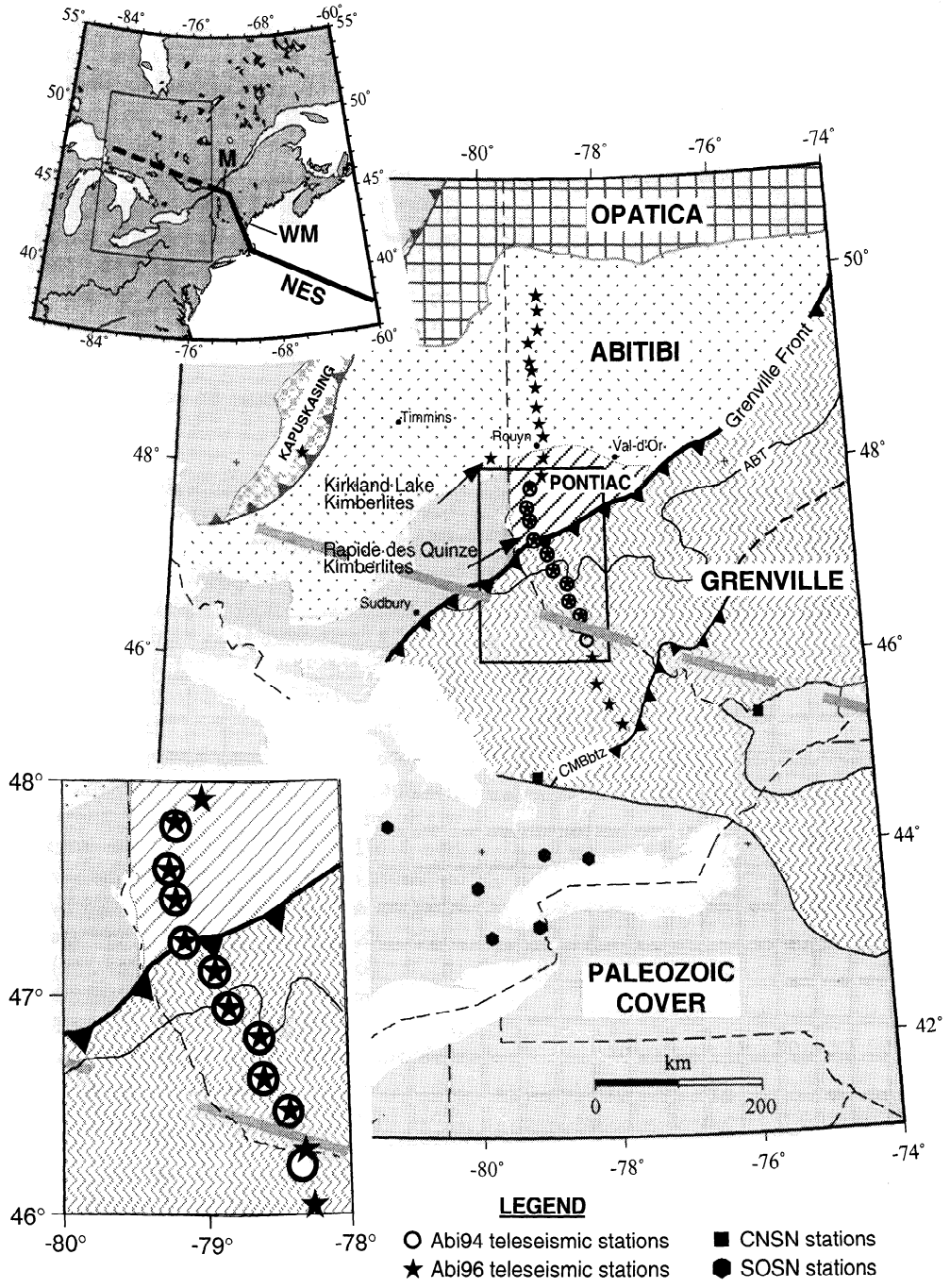

Figure 1. Simplified tectonic map of the study area with the position of teleseismic stations. Top inset shows the location of the study area with respect to central Canada-NE United States; solid line indicates the surface expression of the Monteregian (M)/White Mountains (WM)/New England Seamounts (NES) hotspot track; and dashed line represents the expected hotspot track beneath the Canadian Shield. Bottom inset focuses on the area of the 1994 experiment. ABT, Allochthon Boundary Thrust; CMBbtz, Central Metasedimentary Belt boundary thrust zone.

uity between the two anisotropies as a kinematic indicator manifesting dominantly east-west dextral shearing during this last episode of deformation.

Seismic reflection and refraction profiles indicate substantial variations in Moho depth in the vicinity of the corridor traversed by the teleseismic array. A local thinning of the crust occurs near the latitude of the Grenville Front, where the thickness is 32-34 km, relative to 39-43 km in the Grenville Province, and 34-36 km in the Superior Province [*Winardhi and Mereu,* 1997; *Kellett et al.,* 1994; *Grandjean et al.,* 1995; *Martignole and Calvert,* 1996]. Results of gravity and heat flow surveys [*Mareschal et al.,* 2000; *Antonuk and Mareschal,* 1992; *Guillou et al.,* 1994] show a general

increase in Bouguer gravity anomaly and crustal heat flux from east (Grenville) to west (Kapuskasing). The mantle heat flux is relatively constant across the different provinces and subprovinces of the southeastern Canadian Shield at ~12 mW m^{-2} [*Mareschal et al.*, 2000].

3. Data Acquisition

The data considered in this paper were recorded along two main arrays as part of a two-phase teleseismic survey of the Lithoprobe Abitibi-Grenville transect. Additional recordings from permanent stations located in the study area were included in some of the analyses.

3.1. Abitibi 1994 (Abi94) Experiment

The first temporary array was deployed between July and November 1994 and consisted of 10 short-period seismographs from the French Lithoscope program. Both Hades and Titan data acquisition systems were used to record teleseimic data at 25 Hz and 31.5 Hz sampling rates, respectively. All instruments were connected to portable short-period three-component Lennartz 3D/5s seismometers, with a natural frequency of 0.2 Hz (5 s), permitting recovery of frequencies between 0.2 and 12.5 Hz. The stations were deployed along a NNW-SSE array sampling the Pontiac subprovince and the northern Grenville Province (see bottom inset in Figure 1) at an average spacing of ~25 km. The data collected along this first array have been subject to shear wave splitting [*Sénéchal et al.*, 1996; *Ji et al.*, 1996; *Rondenay et al.*, 2000] and receiver function [*Rondenay et al.*, 2000] analyses.

3.2. Abitibi 1996 (Abi96) Experiment

The second temporary array was deployed between May and November 1996, as part of a collaborative project involving Lithoprobe, the U.S. National Science Foundation (NSF), and the Geological Survey of Canada (GSC). All stations consisted of RefTek data acquisition systems and Streckeisen STS-2 portable three-component broadband seismometers, provided by the Program for Array Seismic Studies of the Continental Lithosphere (PASSCAL) of the Incorporated Research Institutions for Seismology (IRIS). These seismometers have a flat response to ground velocity ranging from 0.0083 to 50 Hz permitting frequency recovery of 0.0083-10 Hz (using a 20-Hz sampling rate). A total of 28 stations were deployed for the Abi96 experiment, 26 of which formed a linear NNW-SSE array which overlapped with the Abi94 line (Figure 1). Stations along the line were spaced at 20-km intervals, and the remaining two stations were deployed west of the main array to allow sampling of the lithosphere below the Kapuskasing Uplift and the Kirkland Lake kimberlite field.

3.3. Permanent Stations

Additional data from the Canadian National Seismograph Network (CNSN) and the Southern Ontario Seismic Network (SOSN) were considered for some of the analyses presented below. The study area includes two CNSN broadband (~0.03-10 Hz) three-component stations, namely, GAC (Glen Almond, Québec) and SADO (Sadowa, Ontario). The SOSN consists of six short-period (1-Hz) three-component stations and is operated by the University of Western Ontario (UWO) for Ontario Hydro.

4. Travel Time Inversion

4.1. Method

Inversion of teleseismic body wave travel times was performed to obtain a velocity model of the upper mantle below the study area. The method used was developed by *VanDecar* [1991] and can be summarized as follows: (1) optimum relative delay times are determined by cross correlation of all pairs of waveforms, for a given event; (2) delay times are inverted for velocity perturbations (with respect to the iasp91 one-dimensional (1-D) radial Earth model [*Kennett and Engdahl*, 1991]) beneath the teleseismic array; (3) the velocity model is parameterized by splines under tension constrained at a grid of regular knots (35×47 knots every 1/2°E-W and 1/3°N-S, respectively, in the horizontal plane, by 27 knots every 25-33 km along the vertical axis), with a region of high resolution bounded by the area of the main location map in Figure 1 and extending from the surface down to 500 km depth; and (4) linear inversion is performed using conjugate gradients [*Hestenes and Stiefel*, 1952], simultaneously solving for slowness perturbation, station time corrections, and event mislocation. The inversion is an iterative damped least squares problem, with regularization by flattening and smoothing (minimizing L_2 norms of first and second model parameter derivatives), and an iterative downweighting of large residuals [*Bostock and VanDecar*, 1995]. Further details are given by *VanDecar* [1991].

4.2. Data Set

The data set for P waves consisted of 2796 travel time picks from 124 events ($5.0 \leq m_b \leq 6.6$; Figure 2a), while for S waves, 918 travel time picks from 40 events ($5.0 \leq m_b \leq 6.6$; Figure 2b) were used. Estimates of relative delay times were obtained from these travel time picks, with average standard deviations of 0.03 s and 0.13 s for P and S waves, repectively. These data did not incorporate seismograms from the Abi94 experiment due to inaccurate timing. The measured delays are mainly from direct P and S phases, but a few core-refracted phases were also included. Both data sets provide reasonable epicentral distance and azimuthal cov-

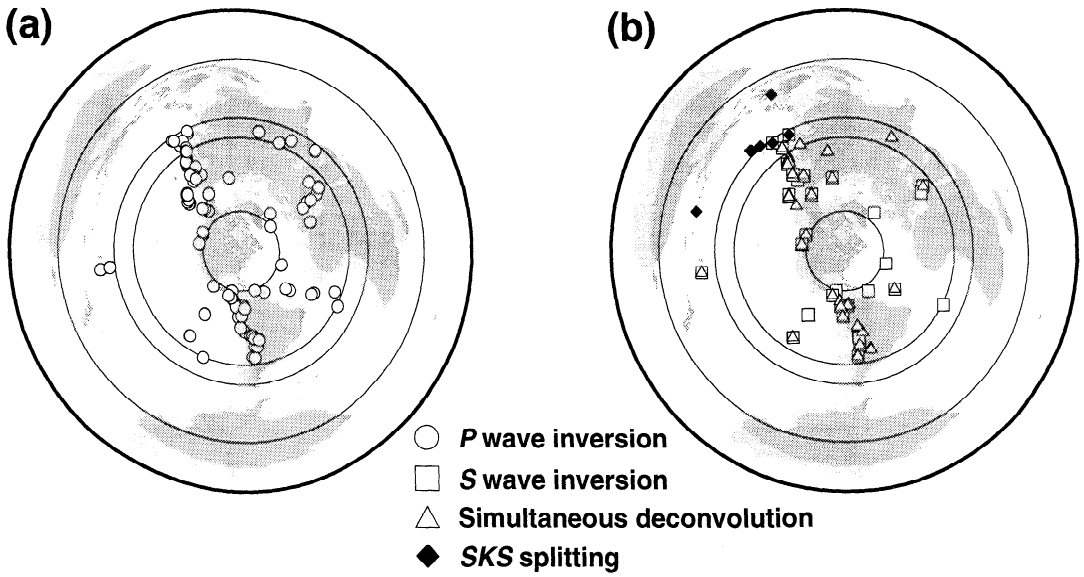

Figure 2. Datasets used for the different analyses performed in this study: (a) P wave travel time inversion; (b) S wave travel time inversion, simultaneous deconvolution, and SKS splitting. See text for details.

erage with, however, a concentration of events located along the edges of the Pacific plate. As a result, there is good ray coverage along a vertical plane coinciding approximately with the teleseismic array.

4.3. Results

The inversion results are presented in Figures 3 and 4 and Plate 1 as horizontal depth slices or vertical profiles through the preferred models. The gray/color scale represents the slowness (reciprocal of velocity) anomaly in terms of percent deviation from the iasp91 radial 1-D model. Regions of poor ray coverage (model parameters sampled by less than four rays) are masked in white on black and white plots (Figures 3 and 4), and in black on colour plots (Plate 1). In all cases shown below, curves representing the trade off between data misfit and model variance were constructed to select the appropriate regularization parameters. Damping parameters were set at 600 (P) and 450 (S) for flattening and 17,200 (P) and 14,100 (S) for smoothing.

A series of resolution tests were performed in order to assess the reliability of our results. These tests involved the construction of synthetic models and calculation of travel time residuals for the same source-receiver combinations as used in the actual inversion. Travel time inversion was then performed, and the resulting models were compared to the original synthetic ones. Figure 3 presents a resolution test performed for synthetic P and S slowness models composed of alternating ($\pm 5\%$) spikes. The 40-km-diameter spherical spikes are positioned at regular intervals within the model volume, and random Gaussian noise (σ=0.03 s for P waves and σ=0.13 s for S waves) has been added to the synthetic travel times. We note that the first layer of spikes (50 km depth) is not well resolved in either P or S inversions. This is explained by the proximity of this layer to the surface; the associated travel time delays are largely absorbed by station static corrections rather than by velocity variations in the model [*VanDecar*, 1991]. For the next three layers (183, 317, and 450 km), the reconstructed image is more consistent with the synthetic input spike model. In the P inversion results, the anomalies are properly positioned within most of the volume illuminated by the rays, a region which near the surface is restricted to a narrow band centered on the array (e.g., ~220 km wide at a depth of 50 km) and widens substantially with depth (e.g., ~800 km at a depth of 300 km). In the S inversion tests the spikes are adequately recovered only directly beneath the teleseismic array, and thus resolution of structure is, not unexpectedly, poorer away from the array axis than for P travel time results. Both P and S wave tests produce amplitudes of recovered spikes that are lower than their original values, and this disparity becomes more pronounced with increasing depth. This observation is explained by (1) the regularization, which favors flatter, smoother solutions over "spiky" ones and (2) the fact that more rays intersect the model points close to the surface than at greater depths, thus placing tighter constraints on amplitudes of the near-surface model perturbations.

The P wave inversion results for the real data are shown in Plate 1; the preferred model explains 93% of the root-mean-square (rms) of P wave delay time re-

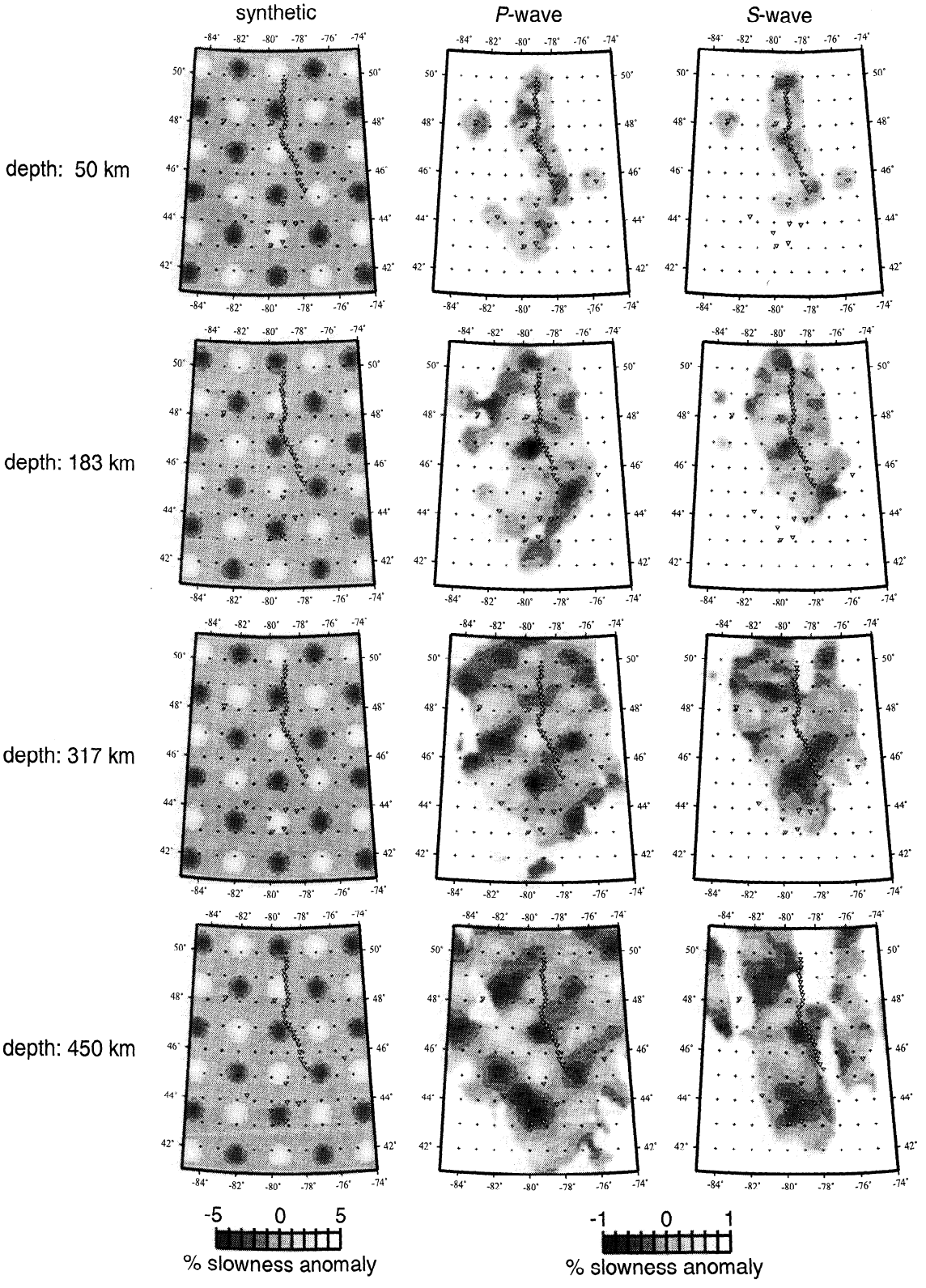

Figure 3. Resolution test for P and S wave travel time inversion. Results are presented as depth slices through the model, with a gray scale giving percent slowness anomaly with respect to iasp91 and regions of poor ray coverage masked in white. (left) Synthetic model, which is composed of alternating $\pm 5\%$ spike anomalies. (middle and right) Inversion results for P and S travel times calculated through the synthetic model. Resolution is generally good within the high ray coverage region, except close to the surface, where some of the variations may be included into station static corrections. We also note that the spikes are better recovered by P than by S travel time inversion, which is probably due to more comprehensive P wave coverage.

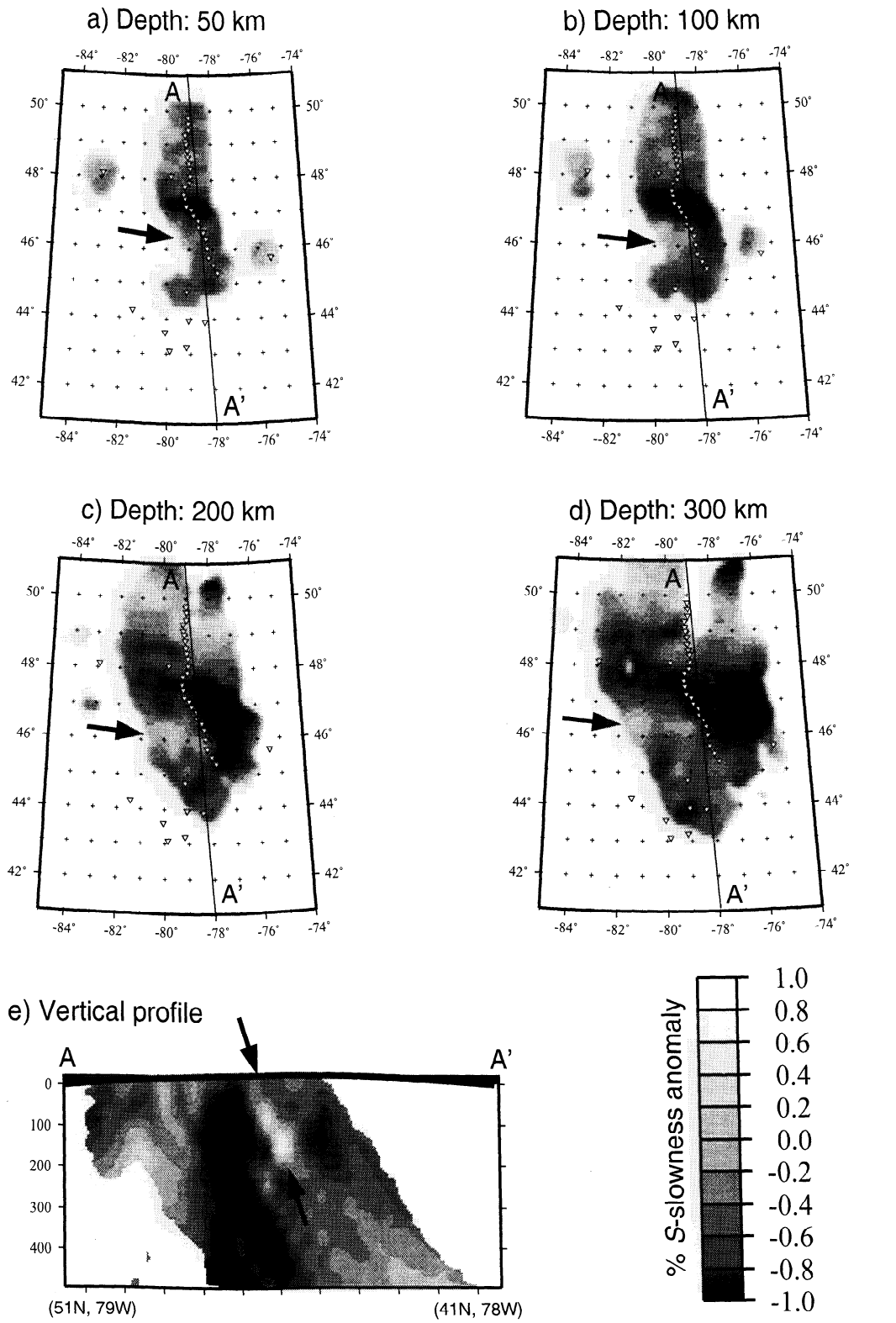

Figure 4. S wave travel time inversion results, presented as (a-d) various horizontal depth slices and (e) a vertical profile through the preferred model. Description of the gray scale is as for Figure 3. A low-velocity anomaly is observed near latitude 46°N, extending mainly west of the station array (see arrows). In this case, the anomaly does not show a clear extension as in the P wave inversion results. This is probably due to the limited data set available for S waves and the resulting loss in resolution.

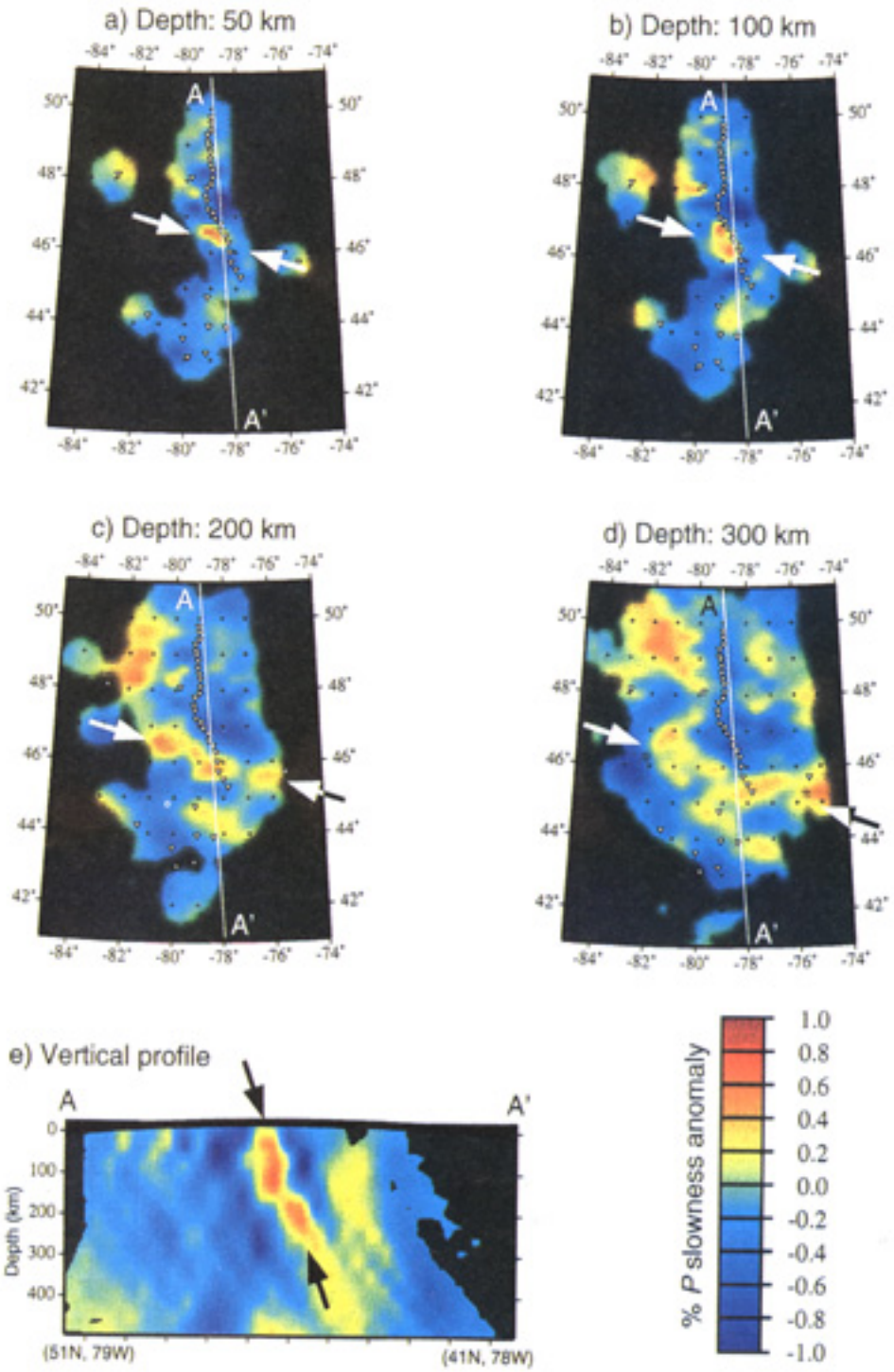

Plate 1. *P* wave travel time inversion results, presented as (a-d) various horizontal depth slices and (e) a vertical profile through the preferred model. The color scale gives the percent slowness anomaly with respect to iasp91, and regions of poor ray coverage are masked in black. A NW-SE trending low-velocity corridor (~1% slowness anomaly; see arrows) is observed, crossing the seismic array near latitude 46°N. The vertical profile shows that the anomaly is nearly vertical and extends between 50 and 300 km depth, with a relatively constant width of ~120 km. At a regional scale the anomaly appears to represent the northwestward extrapolation of the MWN hotspot track. The low-velocity corridor is flanked on either side by two high-velocity anomalies that probably represent the deep lithospheric roots of the Canadian Shield.

siduals (rms reduction from 13.57 to 1.00 s). The most prominent feature to appear on all depth slices is an elongate, positive 1.0% slowness anomaly (low velocity) that crosses the southern portion of the main line near latitude 46°N. As depth increases and the illuminated area widens, the anomaly takes the shape of a NW-SE low-velocity corridor, with an average width of 120 km (measured at 0% slowness anomaly). Plate 1e shows a vertical profile (AA') that cuts the model along the teleseismic array and thus yields an approximately transverse view of the low-velocity corridor. The anomaly dips slightly to the south, which may be due in part to smearing in that direction, and its width remains fairly constant with depth, from 50 to 300 km beneath the surface. Two higher-than-average velocity zones flank the anomaly to the north and south. Synthetic tests and analysis of station corrections demonstrate that the limited outward extent of these features are artificial, reflecting an insensitivity of the method to low wavenumber (including DC) components of structure. Thus the recovered models are band-pass-filtered images of true mantle velocity structure, wherein laterally extended anomalies are well resolved only in the vicinity of more rapid, lateral variations. Accordingly, the high-velocity flanks may persist to the north and south and represent ambient, high-velocity levels of the Canadian Shield, as observed in the North American shear velocity models of *Grand* [1994] and *Van der Lee and Nolet* [1997]. Consequently, the true deviation of the low-velocity zone from ambient mantle may be better represented by a peak to peak anomaly of ~2%.

The S wave inversion results are shown in Figure 4, with the preferred model explaining 97% of the rms of the delay time residuals (rms reduction from 63.97 to 1.64 s). This model also shows the presence of a low-velocity anomaly at the same latitude as that observed for P waves (i.e., near 46°N). However, as expected, the anomaly is less well resolved away from the main axis, especially on the east side of the array. Vertically, the anomaly is better resolved closer to the surface, between 50 and 200 km (see Figure 4e), but the best correlation between the P and S models is obtained around 300 km depth (compare Figure 4d and Plate 1d). Directly north of the low-velocity anomaly, the high-velocity zone observed in the P wave inversion is also present but more extended both horizontally and vertically.

A potential concern regarding the origin of the low-velocity corridor arises from the presence of known Moho topography near its latitude (see section 6). More specifically, a 5-km thickening of the crust from 40 to 45 km in the vicinity above the low-velocity anomaly is followed, to the north, by a shallowing to 35 km depth that coincides with the Grenville Front and the north flanking high-velocity region (see Plates 2 and 3). Contributions to relative travel time residuals of ±0.15s (based on the iasp91 1-D velocity model) might be expected from this structure; however, much of this should be absorbed by station static corrections which are solved for as part of the inversion [*VanDecar,* 1991]. Moreover, velocities above the zone of crustal thinning, as determined from refraction profiling [*Winardhi and Mereu,* 1997], are ~0.3 km/s slower than for the thicker crust to the south, resulting in a vertically integrated net travel time anomaly near zero across the structures. The interplay of crustal thickness and velocity may be responsible for the pattern of static station corrections revealed in Plate 3, where negative values occur at latitudes corresponding to both thinner (~47.3°N) and thicker crust (~46.3°N). However effective static station corrections may be, three independent tests were run to further investigate the influence of strong lateral crustal variations. First, synthetic tests show that Moho relief (without compensating for variation in velocity) does leak some signal into the shallowmost mantle but cannot reproduce the depth nor lateral extent of the low-velocity corridor observed in the tomographic results. Second, we performed a number of "squeezing" inversions [*Lerner-Lam and Jordan,* 1987; *Saltzer and Humphreys,* 1997] using both real and synthetic data (incorporating Moho relief) where different regularizations were imposed to penalize structure at a range of depth intervals within the reconstructed model. Results show that for synthetic data, slowness anomalies associated with crustal structure are concentrated close to the surface (<100 km), whereas the observed data require a majority of the anomaly to reside at depth (100-300 km) within the lithospheric mantle. Third, we performed an inversion from which travel time data from the five stations overlying the mantle slowness anomaly were excluded. Crustal structure at the latitude of the anomaly will thereby have minimal influence on the reconstructed model at mantle lithospheric depths. Our results again indicate a well-defined low-velocity corridor trending NW-SE between 100 and 300 km depth, with average width of 120 km.

5. Shear Wave Splitting Analysis

5.1. Method

Over the past 15 years, numerous studies have demonstrated the global extent of azimuthal seismic anisotropy in the continental lithosphere, which is generally interpreted as due to the lattice preferred orientation of olivine, the primary mineral constituent of the upper mantle [*Babuška and Cara,* 1991; *Vinnik et al.,* 1986; *Silver and Chan,* 1988, 1991]. Azimuthal anisotropy will generally cause a plane-polarized, vertically incident shear wave to split into two quasi shear waves which travel at different velocities and are orthogonally polarized along the principal axes of symmetry. Analysis of shear wave splitting usually assumes propagation through a homogeneous layer, so that anisotropy is parameterized through the following two quantities: (1) the effective polarization direction of the fast wave, ϕ, which is expected to coincide with the direction of crystallographic axis a of olivine, and (2) the effective

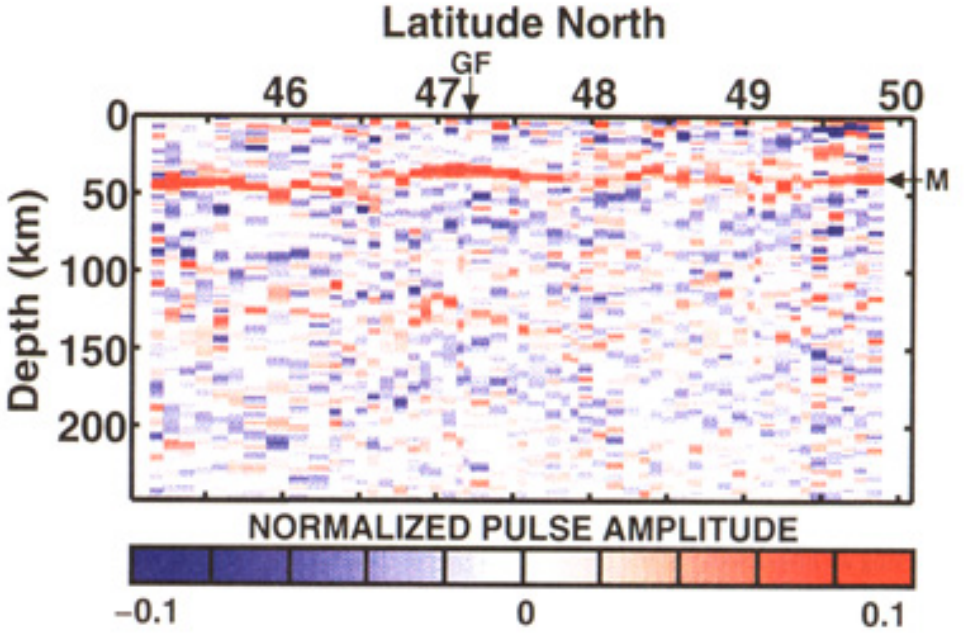

Plate 2. Radial (SV) impulse responses mapped to depth as a function of latitude, binned according to Moho (i.e., 40 km) conversion point. The most prominent feature is the Moho (M), represented by a strong positive polarity pulse, and showing important variations in topography in the vicinity below the surface expression of the Grenville Front (GF). Note jump in Moho depth occuring at ~46.6°N, separating thicker crust to the south (40-45 km) from thinner crust to the north (~35 km).

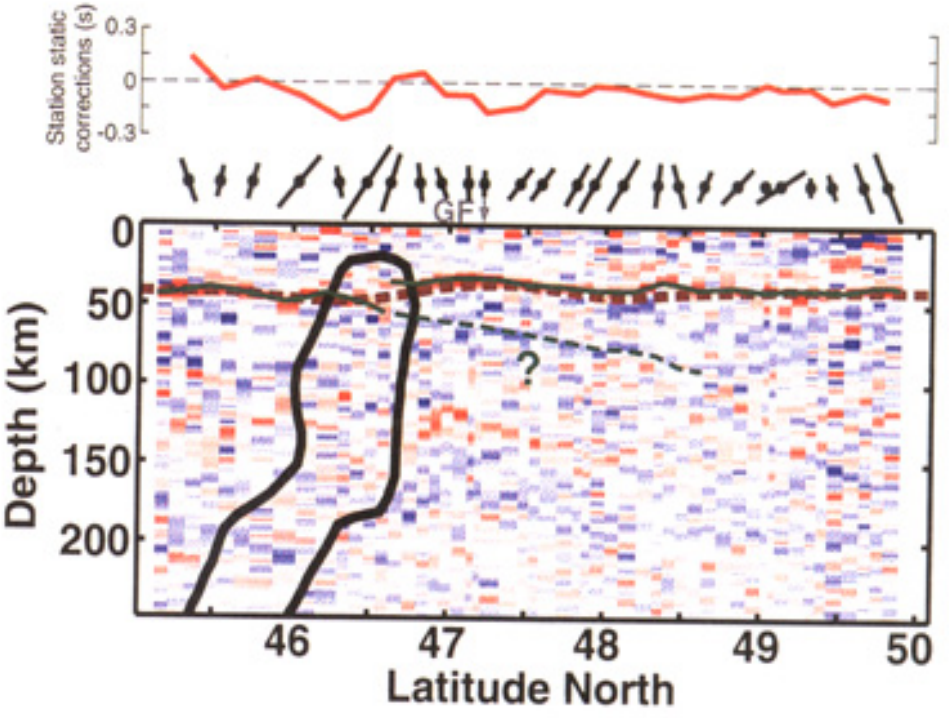

Plate 3. Compilation of the results obtained in this study, with depth to Moho inferred from refraction study [*Winardhi and Mereu*, 1997] indicated by dashed brown line. Background shows the radial impulse response profile (Plate 2), with interpretation of Moho topography shown in green. Dashed green line indicates the presence of a possible subducted plate stranded within the cratonic lithosphere. A cross section of the tomographic low-velocity corridor as defined by the 0% slowness anomaly is outlined in black, and station static corrections are plotted above. Splitting parameters are shown at the position of each station above the profile.

time shift between the fast and slow waves, δt, which is representative of the intensity of anisotropy and the thickness of the anisotropic layer. The *Silver and Chan* [1991] method is employed here to recover the two parameters; in their method an inverse operator is designed that minimizes the transverse energy recorded at the surface (for initial waves of known polarization, i.e., SKS) or the second eigenvalue of a covariance matrix constructed from the two split waves. The method can be extended to treat multiple events simultaneously at a given station [*Wolfe and Silver*, 1998], increasing the robustness of the results with respect to the analysis of single wave forms.

5.2. Data Set

The data set used in this paper consists exclusively of teleseismic SKS phases recorded along the Abi96 array (results from the analysis of the Abi94 data set are given by *Sénéchal et al.* [1996] and *Ji et al.* [1996]). Of 69 events recorded on the Abi96 array with $m_b \geq 5.5$ and minimum epicentral distance of 85° (for which SKS arrives prior to S), only seven events were suitable for shear wave splitting analysis, and all of these occurred in the vicinity of the Sea of Japan (Figure 2b). Furthermore, only subsets of these seven events were considered at each individual station (see "number of events" in Table 1) due to varying levels of noise on the different recordings. Stations such as KAPU and LLAK were affected by generally low SKS signal-to-noise ratio, as evidenced by the fact that only one event could be used in either case.

5.3. Results

Results from multievent SKS splitting analysis of the Abi96 data set are presented in Table 1 and Figure 5. The average value of ϕ over the entire array is N93°E±18°, in agreement with the results from the Abi94 data set, and corresponds to the general trend (E-W, NE-SW) of the main tectonic features at the surface [*Sénéchal et al.*, 1996; *Rondenay et al.*, 2000]. Over the length of the 1996 array, ϕ undergoes a systematic rotation from ENE at the northern stations to ESE in the southern portion of the line, which may be attributed to slight variations in orientation of the last episodes of lithospheric-scale deformation to have affected the area [*Rondenay et al.*, 2000]. Thus anisotropy in the northern portion of the array may reflect E-W regional shear zones of Archean age [*Ji et al.*,

Table 1. Station Locations and Results of SKS Splitting

Site	Latitude °N	Longitude °W	Number of Events	ϕ, deg	δt, s
DEND	49.79	79.01	6	76.00± 8.50	0.90±0.25
VSG4	49.63	79.00	6	77.00±15.50	0.65±0.23
KM44	49.43	79.00	2	79.00±25.50	0.35±0.18
NNNN	49.29	79.16	5	88.00±31.00	0.25±0.20
VBOI	49.10	79.14	4	134.00±13.00	0.55±0.68
VSGL	49.01	79.11	2	53.00± 7.00	0.65±1.60
CHAZ	48.83	79.05	3	120.00±26.50	0.50±0.40
POUL	48.63	79.04	4	104.00±26.00	0.40±0.20
DEST	48.46	79.00	7	80.00±19.50	0.55±0.20
LDUF	48.32	78.94	2	94.00± 8.00	0.55±0.08
KAPU	48.13	82.91	1	49.00±37.50	1.05±0.43
BELL	48.10	78.94	5	110.00±11.00	0.70±0.15
LLAK	48.10	79.80	1	65.00± 6.00	0.65±0.23
CARO	47.92	78.98	4	109.00±13.00	0.75±0.25
POP1	47.81	79.17	5	109.00±28.50	0.55±0.23
POP2	47.59	79.22	2	114.00±13.50	0.45±0.28
POP3	47.45	79.18	5	115.00±29.50	0.45±0.20
POP4	47.22	79.12	3	91.00±14.50	0.35±0.08
POP5	47.12	78.91	4	89.00±16.50	0.45±0.12
POP6	46.95	78.82	5	77.00±27.00	0.40±0.15
POP7	46.81	78.60	5	86.00±22.00	0.50±0.20
POP8	46.62	78.58	5	101.00±20.00	0.75±0.28
POP9	46.47	78.40	5	112.00± 8.50	1.00±0.30
POP10	46.29	78.29	3	83.00±21.50	0.40±0.20
BISC	46.03	78.24	5	110.00±11.00	0.70±0.15
ALQN	45.74	78.19	3	100.00±19.50	0.45±0.10
MADW	45.53	78.00	4	97.00±17.50	0.40±0.10
PAPL	45.32	77.81	2	77.00±16.00	0.55±0.12

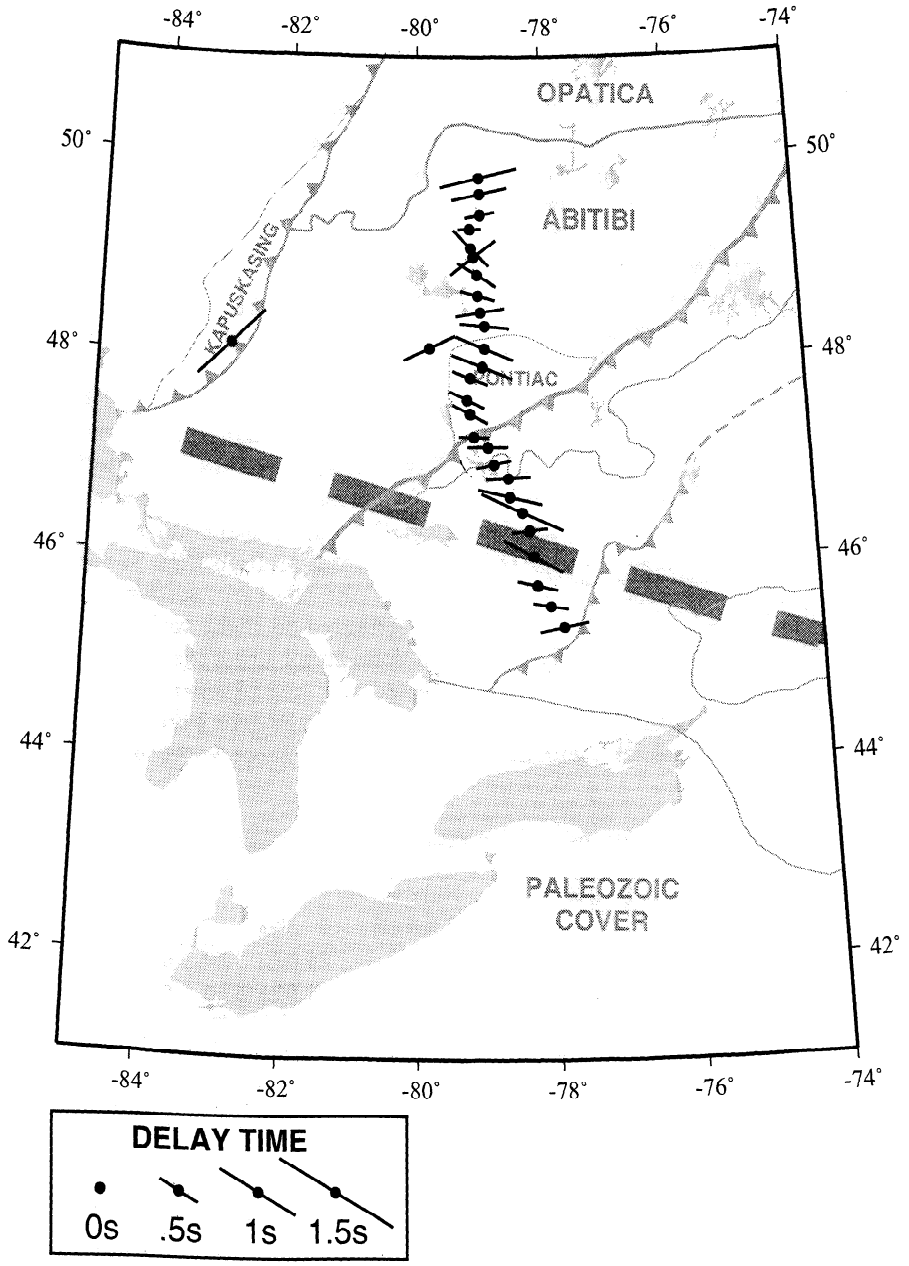

Figure 5. Multievent SKS splitting results. Solid bars indicate the polarization direction ϕ of the fast shear wave, and their lengths are proportional to the delay time δt between the two split waves. The average direction of polarization is E-W and is believed to represent "fossilized" lithospheric strain fields associated with the last major episode of deformation to have affected the region during the Precambrian. Subtle variations in ϕ and δt occur at the latitude of the tomographic low-velocity corridor (~46°N; thick dashed line indicates surface projection of the corridor), providing evidence for complexity in the underlying structure.

1996; *Rondenay et al.*, 2000], whereas in the south it may result from younger regional deformation associated with the Grenvillian Orogeny. In the latter case, fast directions are almost perpendicular to Grenvillian structures (Figure 5), suggesting that the mantle fabric may have recorded the last extensional event of the orogeny (e.g., 1140-1090 Ma [*Carr et al.*, 2000]. Variations in δt from 0.25 to 1.05 s over the entire array (average of 0.57 ± 0.22 s) do not correspond well with previous results [*Rondenay et al.*, 2000]. The inconsistency in magnitude of average δt between the two experiments may be due to the following factors: (1) the difference in back azimuthal coverage (285°-335° for the 1996 experiment, compared to 165°-339° for the 1994 experiment) coupled with depth-dependent and laterally variable anisotropy, which would result in a wider range of delay times for the analysis of the Abi94 data; and (2) the possibility of contamination by source-side

anisotropy introduced through the use of some S and ScS phases in the Abi94 analysis. Subtle variations in ϕ and δt occur at the latitude of the low-velocity corridor (~46°N), providing possible evidence for complexity in the underlying structure (i.e., change in mantle anisotropic fabric).

6. P-S Conversions

6.1. Method

Receiver function analysis is a method commonly used in the study of P to S (Ps) conversions generated at discontinuities in the crust and uppermost mantle [*Langston,* 1979; *Owens et al.,* 1984; *Cassidy,* 1995]. It employs the vertical component of the seismic signal as an estimate of the source and deconvolves it from the radial and transverse components in order to isolate Ps conversions. The approach adopted here contains a series of additional processing steps [*Bostock,* 1998] and can be summarized as follows: (1) the rotated components of the ground displacement vector recorded at the surface [U_R, U_T, U_Z] are transformed into an upgoing wave vector [P, SV, SH] using estimates of near-surface velocities; (2) seismograms are binned in latitude, at selected depth intercepts [e.g., *Dueker and Sheehan,* 1997], in order to better map known discontinuities (Moho, 410, 660), and possible discontinuities within the lithospheric mantle; (3) simultaneous least squares deconvolution of S components by P components is performed in the frequency domain for all seismograms within individual bins to obtain an impulse response; and (4) move-out corrections [*Vinnik,* 1977] calculated using the iasp91 model are applied during deconvolution to coherently stack arrivals from greater depths.

6.2. Data Set

This approach was applied to a joint data set of 568 high-quality seismograms from 49 events, which includes recordings from both Abi96 and Abi94 experiments. The distribution of events is shown in Figure 2b.

6.3. Results

Plate 2 shows the radial impulse responses plotted in color as a function of latitude and binned according to Moho (i.e., 40 km) conversion point. All data have been projected onto a N-S line, and the configuration of the profile is such that two bins separate each pair of stations, with three extra bins (~10km each) added to either end of the station line. The main feature observed on the radial component profile is the Moho, which is represented by a strong positive polarity pulse located at an average depth of 40 km. Moho topography is apparent with a tapered thickening in crust from 40 to 45 km thickness between latitudes 45°N and 46°N followed by an abrupt thinning of crust to ~35 km at 46.6°N. These observations are in good agreement with Moho relief estimated from seismic refraction profiling [*Winardhi and Mereu,* 1997] (see also Plate 3). The refraction Moho in the vicinity of the proposed suture is apparently constrained primarily by refracted waves (versus wide-angle reflections), leading to a smoothing of topographical variations [*Winardhi and Mereu,* 1997]. The scattered wave profile suggests a more discontinuous jump in Moho depth at ~46.6°N, some 65 km south of the Grenville Front. It is important to stress that the image obtained is likely diffuse due to diffraction at the structure. The image might be improved by employing teleseismic migration techniques [*Bostock and Rondenay,* 1999]. However, this is beyond the scope of this paper and may be considered in future processing of this data set. Further interpretation of this Moho jump and its relation to similar features observed on seismic profiles crossing the Grenville Front in other locations are presented in section 7.

A similar analysis (including profiling and stacking) was performed to detect the presence of possible variations in apparent depths to the 410- and 660-km discontinuities. Estimated Ps times from conversions occurring at the 410-km ($P410s$) and 660-km ($P660s$) discontinuities were fairly constant along the entire array at 43.5 and 67.0 s, respectively (compared to theoretical values for iasp91 of 44.1 and 68.1 s). These results are in agreement with those of *Bostock* [1996], suggesting a laterally homogeneous transition zone beneath the study area and below average Ps times related to high-velocity lithospheric mantle beneath the Canadian Shield.

7. Discussion

A compilation of results presented in previous sections is shown in Plate 3 along with the depth to Moho inferred in the study of *Winardhi and Mereu* [1997]. Splitting parameters and station static corrections are shown at the position of each station above the profile. In this section we discuss the tectonic and geodynamic implications of these interpreted lithospheric structures; specifically, the relation of variations in crustal thickness to the Grenvillian Orogeny and the nature of the low-velocity mantle corridor and mechanism responsible for its origin.

7.1. Variations in Crustal Thickness

Our interpretation of Moho topography is shown as a thick green line in Plate 3. The geometry of Moho topography near 46.6°N (i.e., Moho jump, see section 6) is reminiscent of structures observed on a number of high-resolution reflection seismic profiles traversing other Precambrian and Phanerozoic orogens [*Morgan et al.,* 1994; *Calvert et al.,* 1995; *McBride et al.,* 1995; *Warner et al.,* 1996; *Pfiffner et al.,* 1990; *Cook et al.,* 1998]. In many of these studies a tapered crustal thickening followed by abrupt thinning has been ascribed directly to the suture between colliding plates, where the deepening Moho is associated with delaminating continental lower crust on the incoming plate sutured to

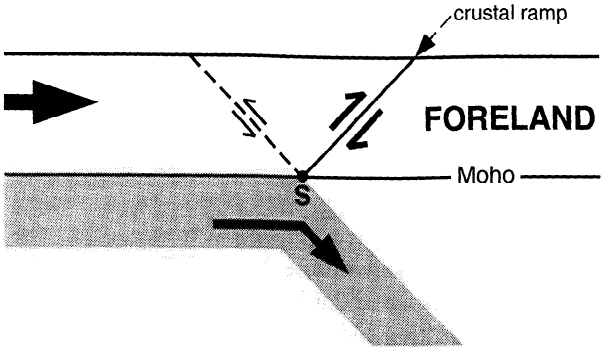

Figure 6. Schematic diagram showing the geometry of a tectonic wedge (modified from *Beaumont and Quinlan* [1994]). The incoming plate on the left is split into an upper section exhumed to the surface along a crustal ramp and a lower section subducted beneath the foreland at point S.

thinner crust on the overriding plate. The results of this process are usually referred to as lithospheric-scale delamination structures or tectonic wedges (Figure 6), since the lithosphere of the incoming plate is effectively split into an upper section exhumed to the surface along a crustal ramp and a lower section subducted beneath the foreland [e.g., *Cook et al.,* 1998]. On the basis of these previous studies a possible interpretation of the Moho jump is a subduction/underthrusting margin within a tectonic wedge whose surface expression is represented by the Grenville Front (i.e., the surficial limit of Grenville deformation), ~65 km to the north. It is further worth noting that a sequence of admittedly weak but suggestive negative polarity arrivals project northward into the mantle from the Moho structure and thus may represent *Ps* conversions from eclogitized oceanic or continental crust stranded within the Superior cratonic lithosphere upon cessation of subduction. As discussed below, our interpretation does not necessarily imply that the Grenville Front is a Grenvillian age suture. In this section we explore the implications of the tectonic wedging hypothesis for the observed Moho structure by focussing on two main points, namely, (1) the relation between the structure and the present location of the Grenville Front and (2) the possible age of the structure.

7.1.1. Moho step and Grenville Front. If subduction/underthrusting is truly responsible for the observed variations in crustal thickness and the location of the Grenville Front as an associated surface feature, a similar signature should be expected at other points along strike of the Grenvillian orogen. A number of other profiles have been run to the southwest and include a refraction line in the Sudbury (Ontario) area [*Winardhi and Mereu,* 1997], and reflection lines in the Great Lakes region (Great Lakes International Multidisciplinary Program on Crustal Evolution [*Green et al.,* 1988]) and Ohio (Consortium for Continental Reflection Profiling [*Culotta et al.,* 1990]). These studies have all involved lines crossing the Grenville Front and all show some evidence for crustal thickening occurring near but on the Grenville side of the Front. Indeed, *Cullotta et al.* [1990] interpret the Ohio profile in terms of subduction but invoke a more complicated two-sided subduction style to explain the doubly-vergent crustal reflections. The formation of tectonic wedges developed through subduction (continental collision or intracontinental compression) has been extensively modeled by *Beaumont and Quinlan* [1994] for a range of physical conditions. In their geodynamic modeling, *Beaumont and Quinlan* [1994] reconsider both the Ohio and Great Lakes profiles in terms of continental collision models with single-sided, northwest dipping subduction. Along strike to the northeast, there are, unfortunately, no reflection profiles which traverse the Grenville Front, but two lines do approach the boundary from the south. *Martignole and Calvert* [1996] identify a ~50-km-wide zone of crustal thinning toward the Front, but this occurs on a portion of the profile oriented largely parallel to orogen strike and thus must represent short-wavelength local structure. *Eaton et al.* [1995], in contrast, document a 10-km crustal thickening toward the Front. Furthermore, a narrow, strike-parallel, negative Bouguer anomaly becomes increasingly evident to the northeast and is generally interpreted to represent locally thickened crust [*Rivers et al.,* 1989]. The peak anomaly is located systematically to the Grenville side of the Front, suggesting that thickening is restricted to Grenville crust and is thus consistent with the model proposed for more southerly portions of the orogen and with a simple subduction margin extending the full length of a paleocraton plate boundary. The intensification in Bouguer anomaly toward the NE portion of the orogen may therefore reflect a more pronounced delamination (wedging) of Grenville crust, perhaps related to an earlier commencement of collision due to geometry of the incoming plate boundary.

7.1.2. Age of subduction. Our next task is to consider the likely age of the proposed tectonic wedge and, in particular, its timing with respect to the Grenvillian Orogeny. We consider three possible scenarios, namely, that the structure is post-, syn-, or pre-Grenvillian.

The possibility of the structure being post-Grenvillian in age is the least likely option, given the lack of physical evidence for a major episode of tectonic activity postdating the orogeny. Indeed, a subduction/suture extending the length of the orogen could not have occurred after the main orogenic pulses without producing important post-Grenvillian reworking of the terranes located southeast of the Grenville Front. Many surface studies conducted in the Grenville Province clearly show that its terranes have retained a metamorphic/deformational inprint dating from the Mesoproterozoic, with no trace of subsequent regional-scale tectonism [*Carr et al.,* 2000, and references therein].

It is widely recognized that the Grenville Front is not a Grenvillian age suture [*Rivers et al.,* 1989; *Rivers,* 1997], or at least not one which was originally activated syntectonically with the main orogenic pulses. Numerous geological and geophysical studies have outlined the extent of reworked Archean rocks as far as 200 km south of the Grenville Front [*Martignole and Calvert,* 1996; *Dickin and McNutt,* 1989; *Rivers,* 1997, and references therein]. Furthermore, there is geochronologic and isotopic evidence for an Andean-style subduction margin along southeastern Laurentia, in effect over a period of ~500 Myr between 1.71 and 1.23 Ga [*Rivers,* 1997]. At that time, the Laurentian margin between southeastern Ontario and Labrador was located up to 600 km southeast of the present location of the Grenville Front [*Rivers,* 1997; *Rivers and Corrigan,* 2000]. Thus, at the onset of the Grenvillian Orogeny, a major portion of the Laurentian continent extended well into the present-day Grenville Province, implying that the tectonic wedge proposed in this study could not have been the result of a contemporary suture. However, the wedge could be related to a pre-Grenvillian suture reactivated during the last pulse of the northwest propagating orogeny. A related model involving step-up shear zone and associated intra-continental subduction/underthrusting has been suggested for the Grenville Front Tectonic Zone in NE Ontario [*Haggart et al.,* 1993], using geochronological results and geodynamic models of *Beaumont and Quinlan* [1994]. In a more general sense, several authors have tentatively interpreted the Grenville Front as a reactivated zone of weakness that was originally associated with the buildup of Laurentia [*Martignole and Calvert,* 1996; *White et al.,* 2000; *Holmden and Dickin,* 1995]. A similar form of intra-continental reworking due to the reactivation of long-lived (possibly accretion related) structures has been inferred from seismic profiles across the Arunta Block in central Australia [*Goleby et al.,* 1989; *Kosch et al.,* 1998].

On the basis of the arguments presented above, we propose the existence of an active continental margin that predated the Grenvillian orogen and approximately paralleled its northwesternmost boundary. This margin would have been instrumental in defining the location of the Grenville Front, by providing a pre-existing lithospheric ramp for the exhumation of lower crustal elements towards the surface. The Moho step would thus represent a relict subduction margin, possibly reactivated as an underthrust sheet during the Grenvillian orogeny. To the southwest of the Great Lakes, the inferred subduction may have coincided with the Mesoproterozoic active margin of Laurentia, since arc magmatism of that age has been identified in the Proterozoic foreland of the orogen [*Rivers and Corrigan,* 2000]. The absence of systematic foreland arc magmatism over the full extent of the Greville Front remains problematic but might be explained by varying subduction geometry along the margin, as is documented on the western margin of South America [*Sacks,* 1983].

7.2. Nature of the Low-Velocity Mantle Corridor

An outline of the low-velocity mantle corridor, as defined by the 0% slowness anomaly contour and determined from inversion of P wave travel time delays, is presented in Plate 3. The essential geometrical characteristics of this feature that must be considered in assessing its physical significance are as follows: (1) it is quasi-linear in planform and strikes NW-SE; (2) it is constrained to the mantle above at most 300 km depth; and (3) it is <120 km in cross-strike width. The trend of the structure is well resolved (see dashed line in Figure 1) as highly oblique to the NE-SW strike of the Grenville Orogen, thus rendering an association between the two features unlikely. Rather, the geometry of the low-velocity corridor is better correlated with an extrapolation of structures associated with more recent tectonic activity, namely, the alkaline volcanism which defines the MWN hotspot track and the Kirkland Lake-Rapide des Quinze kimberlite fields (Figure 1). It is this interpretation which we shall pursue in more detail by first considering the process responsible for these surficial features and then the possible factors contributing to low mantle velocities.

7.2.1. Proposed mechanisms for the MWN track. Two different processes have been proposed to explain magmatism along the hotspot track, namely, (1) a fixed mantle plume and (2) an episode of continental rifting. The plume hypothesis is based on five main arguments. First, the geographical configuration of the MWN Cretaceous formations and a possible relation with the North American plate drifting over a fixed mantle plume were originally proposed by *Morgan* [1972], mainly based on the geographical succession of these linear chains [see also *Morgan,* 1971]. Second, radiometric ages show a clear age progression along the New England Seamounts (83-119 Ma, from east to west [*Duncan,* 1984]) and between the other groups, which are dated at 100-125 Ma for the Cretaceous White Mountains [*Foland and Faul,* 1977] and at 124 Ma for the Monteregian Hills (single pulse [*Foland et al.,* 1986]). Similar dates from earlier studies were compiled by *Crough* [1981] and allowed him to trace the plume back to its present location, that of the Great Meteor hotspot (~30°N, 30°W). Third, the spatiotemporal coordinates of the Kirkland Lake and Rapide des Quinze kimberlite fields are in agreement with the continental drift rate of North America proposed for middle to late Mesozoic time [*Crough et al.,* 1980; *Crough,* 1981; *Duncan,* 1984]. Fourth, the evidence of hotspot-related uplift along the continental portion of the track was reported and analyzed by *Crough* [1981], and the swell of the marine portion was studied by *Sleep* [1990b]. Fifth, a similarity of initial Sr and Nd isotopic ratios between the land and sea portions of the track suggests the mantle plume origin, as noted by *Foland et al.* [1988].

The effect of a mantle plume on the lithosphere has been examined by several authors [*Crough,* 1981; *Sleep,*

1990a, 1996, 1997; *Duncan and Richards,* 1991; *Davies,* 1994]. *Davies* [1994] described a process of thermomechanical erosion which involves heating-softening of the lithospheric base by a plume tail, followed by mechanical removal of the material due to convective transfer. In the case of thick continental lithosphere, *Davies* [1994] estimated that the time of contact with a plume tail necessary to obtain partial melting is ~25 Myr. For the present study area it would have taken at least 25 Myr for the plume to produce the track of 600 km from its westernmost point (~150 Ma emplacement of the Kirkland Lake kimberlites) to the Monteregian Hills (124 Ma). In that case, any point at the base of the lithosphere beneath the study area would have been in contact with the plume tail for no longer than 5 Myr (for a 120-km-diameter plume tail). This time is inadequate for partial melting to occur and would explain the lack of obvious surficial expression on the Canadian Shield.

The continental rifting hypothesis, on the other hand, is supported by four main arguments. First, the different Cretaceous formations of eastern North America coincide with the trend of rift zones that may have been activated or reactivated in relation to the opening of the Atlantic Ocean [*Kumarapeli,* 1976; *Sykes,* 1978; *McHone and Butler,* 1984; *Bédard,* 1985; *McHone,* 1996; *Faure et al.*, 1996]. Indeed, the Monteregian Hills are located near the junction of the Ottawa-Bonnechere Graben, which is believed to be of late Precambrian age but would have been reactivated during the Mesozoic, and the St. Lawrence Valley Paleozoic rift system [*Kumarapeli,* 1976; *Sykes,* 1978; *Bédard,* 1985]. The New England Seamounts are considered by some authors as being related to the early Jurassic Kelvin Fracture Zone, again associated with the opening of the North Atlantic [*Sykes,* 1978; *Bédard,* 1985]. Second, even if the White Mountains are not located above a well-defined rift structure, they still show different episodes of magmatism, with three main pulses at 230 Ma, at 200-165 Ma, and in the Cretaceous at 125-100 Ma [*Foland and Faul,* 1977]. The Early Jurassic middle pulse corresponds to the initiation of rifting between North America and Africa. Furthermore, there are strong geochemical similarities between formations associated with different pulses [*McHone,* 1996]. Hence *McHone* [1996] argues that a long-lived lithospheric tectonic zone is better suited to explain the geographical overlap of similar magmas of different ages. Moreover, *Bédard* [1985] argues that the doming (or uplift) observed in eastern North America is associated with the first main pulse of magmatism of this continental rift system, rather than to the younger Cretaceous alkaline formations. Third, only the New England Seamounts show a clear age progression among individual volcanic centers [*Bédard,* 1985; *McHone,* 1996]. Fourth, a paleostress study conducted by *Faure et al.* [1996] outlines two important events with contrasting extension direction during the Cretaceous: (1) an early regional NE-SW directed extension at ~140 Ma, which would have reactivated the Ottawa-Bonnechere Graben and extended farther west in the Canadian Shield to induce kimberlite magmatism; and (2) younger, localized N-S directed extension, at 125 Ma, which would have been generated as a response to the earlier event and is responsible for the single pulse of magmatism leading to the Monteregian Hills.

The effect of rifting on a thin continental plate is one of extension accompanied by decompressional melting at the base of the lithosphere, producing magmatic episodes at the surface [*White and Mc Kenzie,* 1989; *Bédard,* 1985]. Within the thicker lithosphere of the Canadian Shield, events of tensional stress like the one discussed by *Faure et al.* [1996] could produce some extension, generating occasional kimberlite volcanism without major uprise of decompressional melt.

7.2.2. Physical properties and low velocity. We now consider the nature of the seismic anomaly observed beneath the study area by discussing the possible factors contributing to low mantle velocities, specifically: (1) temperature, (2) composition, and (3) mineral fabric/anisotropy. It must be recognized, at the outset, that images in Plate 1 likely represent minimum estimates of true mantle velocity contrasts as a result of the smoothing/damping equations which are applied to regularize the inverse problem. Thus, on the basis of synthetic tests a peak to peak anomaly of 1-2% may manifest a true velocity contrast of 3-4%. Experimental temperature derivatives of seismic velocities show that P velocity anomalies of this order are produced by 400-600 K perturbations [*Kumazawa and Anderson,* 1969; *Sobolev et al.,* 1996]. This may appear unrealistically large given that such elevated temperatures would inevitably intersect the solidus in some areas, implying large-scale generation of partial melt. By incorporating temperature-induced effects on anharmonicity, mineral reactions, anelasticity, and production of partial melt and their influence on seismic velocities, *Sobolev et al.* [1996] argue that smaller temperature perturbations of order 100-200 K may suffice to explain a 3% velocity variation. The presence of kimberlites erupted at 158-126 Ma requires that the underlying mantle must have been subject to thermal perturbations in the past; however, a major present-day thermal contribution to the observed anomaly is judged unlikely on several grounds. First, the anomaly width is of order 120 km, and for heat not to have diffused to greater extent over a period of ~150 Myr would require the initial thermal disturbance to have occurred along an exceedingly narrow zone (i.e., fracture). Moreover, this disturbance would have to be maintained over an unrealistically long time period to produce a measurable anomaly in the present day. In addition, a local heat flow anomaly would be expected over the feature, whereas none has been thus far observed [*Mareschal et al.,* 2000]. For these reasons we dismiss the notion that a present-day major thermal anomaly is responsible for the low-velocity cor-

ridor. However, we retain for consideration the possibility of contributions from minor thermal perturbations (i.e., remnant; <100 K) with related anelasticity, anharmonicity, and mineral reactions (e.g., metasomatism). A second viable mechanism is the current existence of small pockets of melt within the lithosphere formed through minor degrees of decompression, as contemporary stress fields appear to produce maximum horizontal extension with a component perpendicular to the strike of the Ottawa-Bonnechere Graben [*Zoback,* 1992].

Compositional changes can also produce variations in velocity. In this case, the most important factor is usually considered to be Fe content, with fertile (Fe-rich) mantle peridotite exhibiting reduced velocity relative to more depleted rock [e.g., *Jordan,* 1978, 1979]. In the context of the low-velocity anomaly observed here, Fe-rich magmas may have penetrated the lithosphere through either fracturing or thermomechanical erosion and may have solidified along a narrow fracture system and/or a thermomechanically eroded plume channel. However, the velocity variations associated with Fe content (and those ascribed to different rock types, i.e., eclogite versus peridotite) are generally considered not to exceed 1% in magnitude [e.g., *Jordan,* 1979; *Anderson,* 1990; *Sobolev et al.,* 1996]). Thus compositional changes cannot be wholly responsible for the tomographic anomaly.

Changes in anisotropic parameters represent a major source of velocity variation within the continental lithospheric mantle [*Anderson,* 1990] and may be in major part responsible for the low-velocity corridor observed beneath the Canadian Shield. Some evidence for this comes from the variation in splitting parameters over the vicinity of the anomaly, which presumably betrays a change in configuration of mantle fabric (Figure 5), although a potential anisotropic structure of stranded former oceanic lithosphere dipping to the NW near the tomographic anomaly must also be acknowledged. An origin in anisotropy might tend to favor the rifting hypothesis for the MWN track through attendent rheological considerations; however, it is also conceivable that thermomechanical erosion as envisaged by *Davies* [1994] could promote mineral alignment.

The analysis remains somewhat inconclusive as a clearly superior candidate for the physical property of the anomaly fails to emerge. On the basis of simple conduction models it appears unlikely that the anomaly could represent a thermal signature directly associated with the process responsible for MWN magmatism; however, minor degrees of decompressional melting, composition, and anisotropy remain as potential contenders. The narrow width of the anomalous corridor would further appear to favor continental rifting over plume-induced thermomechanical erosion as a viable mechanism of origin. It is, nevertheless, difficult to ignore the arguments summarized earlier which favor the latter explanation, and some form of mantle plume interaction is clearly required to faithfully accommodate all constraints. An interesting hybrid model which involves both elements has been proposed recently by *Ebinger and Sleep* [1998] to explain continental magmatism and uplift throughout East Africa. Magmatism there occurs along rift zones, with gravity, geochemical data, and small degrees of extension all pointing toward plume-related volcanism [*Ebinger and Sleep,* 1998, and references therein]. They show that a single, large plume can explain the timing and location of volcanism in the area, provided that plume material reaches the surface and/or preferentially causes uplift in regions of thinned lithosphere associated with preexisting continental rifts [see also *Sleep,* 1996, 1997]. These results are readily adapted to the present work by observing the alignment of the low-velocity corridor with several ancient (Paleozoic) rift systems. Early rifting episodes would likely have weakened and locally thinned the base of the lithosphere beneath the Canadian Shield. Small degrees of partial melt created during subsequent passage of the North American plate over a fixed mantle plume (i.e., that responsible for the Great Meteor hotspot) would naturally migrate into these zones, interacting with continental lithosphere to produce localized kimberlite in thick cratonic areas and more regular, linear igneous series in peripheral regions.

8. Concluding Remarks

The results presented here highlight the importance of two processes fundamental in shaping the character of the cratonic lithosphere, namely, (1) subduction associated to the assembly of continental blocks, and (2) modification of the craton edifice through rifting and plume-lithosphere interaction. More specifically, the Grenville Front is interpreted to represent the surface limit of a pre-Grenvillian zone of tectonic wedging/indentation between two continental blocks formerly separated by NW dipping subduction. Gravity data and seismic profiles crossing other portions of the Grenville Front suggest that the lithospheric wedge may be ubiquitous over the entire length of the exposed orogen. In addition, we present evidence that mechanisms responsible for linear anorogenic volcanic chains in thinner continental and oceanic lithospheres are also likely to leave an imprint within thicker cratonic edifices. While previous studies have extrapolated hotspot tracks in areas of thick lithosphere using surface observations of rare kimberlitic intrusions, the results obtained here provide a more direct link between an extensively documented hotspot track and a well-resolved low-velocity corridor underneath the Canadian Shield. Plume-lithosphere interaction is implied on the basis of age progression and geochemistry, but a more precise understanding of the process will await targeted 2-D regional studies of these structures.

Acknowledgments. The authors acknowledge everybody at IRIS PASSCAL(LDEO) and DMC, the Geological

Survey of Canada, J. Goutier at MRNQ, and graduate students at EPM and NMSU for making the Abitibi 1996 field experiment possible. We also thank R. Mereu and B. Dunn (UWO) for access to the SOSN data; J. VanDecar for his travel time inversion code; and C-G Bank for all his help. The authors made use of the Generic Mapping Tools (GMT [*Wessel and Smith*, 1995]) for some of the figures. The original manuscript was greatly improved through discussions with Beckie Jamieson and Chris Beaumont and constructive reviews by Dave Eaton, Justin Revenaugh and Susan Schwartz. Supported by graduate scholarships from the Natural Science and Engineering Research Council of Canada and the "Fonds pour la Formation de Chercheurs et l'Aide à la Recherche" (Québec) to S.R. and a grant from the National Science Foundation (Division of International Programs 9322499) to T.M.H. Lithoprobe publication 1123.

References

Adams, J., and P. Basham, The seismicity and seismotectonics of eastern Canada, in *Neotectonics of North America*, edited by D. B. Slemmons et al., pp. 261-276, Geol. Soc. of Am., Boulder, Colo., 1991.

Anderson, D. L., Geophysics of the continental mantle: an historical perspective, in *Continental Mantle*, edited by M. A. Menzies, pp. 1-30, Clarendon, Oxford, England, 1990.

Anderson, D. L., The scales of mantle convection, *Tectonophysics, 284*, 1-17, 1998.

Antonuk, C. N., and J. C. Mareschal, Preliminary gravity modelling along the Lithoprobe seismic reflection profiles 28 and 29, northern Abitibi Subprovince, in *Proceedings, Lithoprobe Abitibi-Grenville Transect, Rep. 33*, pp. 71-75, Lithoprobe, Vancouver, B.C., 1992.

BABEL Working Group, Evidence for early Proterozoic plate tectonics from seismic reflection profiles in the Baltic shield, *Nature, 348*, 34-38, 1990.

Babuška, V., and M. Cara, *Seismic Anisotropy in the Earth*, 217 pp., Kluwer Acad., Norwell, Mass., 1991.

Beaumont, C., and G. Quinlan, A geodynamic framework for interpreting crustal-scale seismic-reflectivity patterns in compressional orogens, *Geophys. J. Int., 116*, 754-783, 1994.

Bédard, J. H., The opening of the Atlantic, the Mesozoic New England Igneous Province, and mechanisms of continental breakup, *Tectonophysics, 113*, 209-232, 1985.

Benn, K., E. W. Sawyer, and J.-L. Bouchez, Orogen parallel and transverse shearing in the Opatica belt, Quebec: Implications for the structure of the Abitibi Subprovince, *Can. J. Earth Sci., 29*, 2429-2444, 1992.

Bostock, M. G., A seismic image of the upper mantle beneath the North American craton, *Geophys. Res. Lett., 23*(13), 1593-1596, 1996.

Bostock, M. G., Mantle stratigraphy and evolution of the Slave province, *J. Geophys. Res., 103*, 21,183-21,200, 1998.

Bostock, M. G., and S. Rondenay, Migration of scattered teleseismic body waves, *Geophys. J. Int., 137*, 732-746, 1999.

Bostock, M. G., and J. C. VanDecar, Upper mantle structure of the northern Cascadia subduction zone, *Can. J. Earth. Sci., 32*, 1-12, 1995.

Burke, K. C., and J. T. Wilson, Hot spots on the Earth's surface, *Sci. Am., 235*(2), 46-57, 1976.

Calvert, A. J., E. W. Sawyer, W. J. Davis, and J. N. Ludden, Archaean subduction inferred from seismic images of a mantle suture in the Superior Province, *Nature, 375*, 670-673, 1995.

Card, K. D., and A. Ciesielski, DNAG No. 1: Subdivisions of the Superior Province of the Canadian Shield, *Geosci. Can., 13*, 5-13, 1986.

Carr, S. D., R. M. Easton, R. A. Jamieson, and N. G. Culshaw, Geologic transect across the Grenville Orogen of Ontario and New York, *Can. J. Earth Sci.*, in press, 2000.

Cassidy, J. F., Review: Receiver function studies in the southern Canadian Cordillera, *Can. J. Earth Sci., 32*, 1514-1519, 1995.

Clowes, R. M., Lithoprobe phase IV: Multidisciplinary studies of the evolution of the continent–A progress report, *Geosci. Can., 23*, 109-123, 1997.

Cook, F. A., A. J. van der Velden, K. W. Hall, and B. J. Roberts, Tectonic delamination and subcrustal imbrication of the Precambrian lithosphere in northwestern Canada mapped by Lithoprobe, *Geology, 26*, 839-842, 1998.

Crough, S. T., Mesozoic hotspot epeirogeny in eastern North America, *Geology, 9*, 2-6, 1981.

Crough, S. T., W. J. Morgan, and R. B. Hargraves, Kimberlites: Their relation to mantle hotspots, *Earth Planet. Sci. Lett., 50*, 260-274, 1980.

Culotta, R. C., T. Pratt, and J. Oliver, A tale of two sutures: COCORP's deep seismic surveys of the Grenville province in the eastern U.S. midcontinent, *Geology, 18*, 646-649, 1990.

Currie, K. L., *The Alkaline Rocks of Canada*, 228 pp., GSC bulletin 239, Ottawa, Ont., 1976.

Davies, G. F., Thermomechanical erosion of the lithosphere by mantle plumes, *J. Geophys. Res., 99*, 15,709-15,722, 1994.

De Wit, M., C. Roehring, R. J. Hart, R. A. Armstrong, C. E. J. de Ronde, R. W. E. Green, M. Tredoux, E. Peberdy, and R. A. Hart, Formation of an Archaean continent, *Nature, 357*, 553-562, 1992.

Dickin, A. P., and R. H. McNutt, Nd model age mapping of the southeast margin of the Archean foreland in the Grenville province of Ontario, *Geology, 17*, 299-302, 1989.

Dueker, K. G., and A. F. Sheehan, Mantle discontinuity structure from midpoint stacks of converted P to S waves across the Yellowstone hotspot track, *J. Geophys. Res., 102*, 8313-8327, 1997.

Duncan, R. A., Age progressive volcanism in the New England seamounts and the opening of the central Atlantic Ocean, *J. Geophys. Res., 89*, 9980-9990, 1984.

Duncan, R. A., and M. A. Richards, Hotspots, mantle plumes, flood basalts, and true polar wander, *Rev. Geophys., 29*(1), 31-50, 1991.

Eaton, D. W., A. Hynes, A. Indares, and T. Rivers, Seismic images of eclogites, crustal-scale extension, and Moho relief in the eastern Grenville Province, Quebec, *Geology, 23*, 855-858, 1995.

Ebinger, C. J., and N. H. Sleep, Cenozoic magmatism throughout east Africa resulting from impact of a single plume, *Nature, 395*, 788-791, 1998.

Faure, S., A. Tremblay, and J. Angelier, State of intraplate stress and tectonism of northeastern America since Cretaceous times, with particular emphasis on the New England-Quebec igneous province, *Tectonophysics, 255*, 111-134, 1996.

Foland, K. A., and H. Faul, Ages of the White Mountain intrusives–New Hampshire, Vermont, and Maine, USA, *Am. J. Sci., 277*, 888-904, 1977.

Foland, K. A., L. A. Gilbert, C. A. Sebring, and J.-F. Chen, $^{40}Ar/^{39}Ar$ ages for plutons of the Monteregian Hills, Quebec: Evidence for a single episode of Cretaceous magmatism, *Geol. Soc. Am. Bull., 97*, 966-974, 1986.

Foland, K. A., J.-F. Chen, L. A. Gilbert, and A. W. Hofmann, Nd and Sr isotopic signatures of Mesozoic plutons in northeastern North America, *Geology, 16*, 684-687, 1988.

Goleby, B. R., R. D. Shaw, C. Wright, B. L. N. Kennett, and K. Lambeck, Geophysical evidence for 'thick-skinned' crustal deformation in central Australia, *Nature, 337*, 325-330, 1989.

Grand, S. P., Mantle shear structure beneath the Americas and surrounding oceans, *J. Geophys. Res., 99*, 11,591-11,621, 1994.

Grandjean, G., H. Wu, D. J. White, M. Mareschal, and C. Hubert, Crustal velocity models for the Archean Abitibi greenstone belt from seismic refraction data, *Can. J. Earth Sci., 32*, 149-166, 1995.

Green, A. G., B. Milkereit, A. Davidson, C. Spencer, D. R. Hutchinson, W. F. Cannon, M. W. Lee, W. F. Agena, J. C. Behrendt, and W. J. Hinze, Crustal structure of the Grenville Front and adjacent terranes, *Geology, 16*, 788-792, 1988.

Guillou, L., J.-C. Mareschal, C. Jaupart, C. Gariépy, G. Bienfait, and R. Lapointe, Heat flow, gravity and structure of the Abitibi belt, Superior Province, Canada: Implications for mantle heat flow, *Earth Planet. Sci. Lett., 122*, 103-123, 1994.

Haggart, M. J., R. A. Jamieson, P. H. Reynolds, T. E. Krogh, C. Beaumont, and N. G. Culshaw, Last gasp of the Grenville Orogeny: Thermochronology of the Grenville Front tectonic zone near Killarney, Ontario, *J. Geol., 101*, 575-589, 1993.

Hestenes, M. R., and E. Stiefel, Methods of conjugate gradients for solving linear systems, *Nat. Bur. Standards J. Res., 49*(6), 409-436, 1952.

Hoffman, P. F., United plates of America, The birth of a craton: Early Proterozoic assembly and growth of Laurentia, *Annu. Rev. Earth Planet. Sci., 16*, 543-603, 1988.

Hoffman, P. F., Geological constraints on the origin of the mantle root beneath the Canadian Shield, *Philos. Trans. R. Soc. London, Ser. A, 331*, 523-532, 1990.

Holmden, C., and A. P. Dickin, Paleoproterozoic crustal history of the southwestern Grenville Province: Evidence from Nd isotopic mapping, *Can. J. Earth Sci., 32*, 472-485, 1995.

Ji, S., S. Rondenay, M. Mareschal, and G. Sénéchal, Obliquity between seismic and electrical anisotropies as a potential indicator of movement sense for ductile shear zones in the upper mantle, *Geology, 24*, 1033-1036, 1996.

Jordan, T. H., Composition and development of the continental tectosphere, *Nature, 274*, 544-548, 1978.

Jordan, T. H., Mineralogies, densities and seismic velocities of garnet lherzolites and their geophysical implications, in *The Mantle Sample: Inclusions in Kimberlites and Other Volcanics, Proceedings of the Second International Kimberlite Conference*, vol. 2, edited by F. R. Boyd and H. O. A. Meyer, pp. 1-14, AGU, Washington, D.C., 1979.

Kellett, R. L., A. E. Barnes, and M. Rive, The deep structure of the Grenville Front: A new perspective from western Quebec, *Can. J. Earth Sci., 31*, 282-292, 1994.

Kennett, B. L. N., and E. R. Engdahl, Traveltimes for global earthquake location and phase identification, *Geophys. J. Int., 105*, 429-465, 1991.

Kimura, G., J. N. Ludden, J.-P. Desrochers, and R. Hori, A model of ocean-crust accretion for the Superior province, Canada, *Lithos, 30*, 337-355, 1993.

Korsch, R. J., B. R. Goleby, J. H. Leven, and B. J. Drummond, Crustal architecture of central Australia based on deep seismic reflection profiling, *Tectonophysics, 288*, 57-69, 1998.

Kumarapeli, P. S., The St. Lawrence rift system, related metallogeny, and plate tectonic models of appalachian evolution, in *Metallogeny and Plate Tectonics, Geol. Assoc. Can. Spec. Pap., 14*, 301-320, 1976.

Kumazawa, M., and O. L. Anderson, Elastic moduli, pressure derivatives, and temperature derivatives of single-crystal olivine and single-crystal forsterite, *J. Geophys. Res., 74(25)*, 5961-5972, 1969.

Langston, C. A., Structure under Mount Rainier, Washington, inferred from teleseismic body waves, *J. Geophys. Res., 84*, 4749-4762, 1979.

Lerner-Lam, A. L., and T. H. Jordan, How thick are the continents?, *J. Geophys. Res., 92*, 14,007-14,026, 1987.

Ludden, J., and C. Hubert, Geologic evolution of the Late Archean Abitibi greenstone belt of Canada, *Geology, 14*, 707-711, 1986.

Mareschal, M., R. L. Kellet, R. D. Kurtz, J. N. Ludden, S. Ji, and R. C. Bailey, Archaean cratonic roots, mantle shear zones and deep electrical anisotropy, *Nature, 375*, 134-137, 1995.

Mareschal, J. C., C. Jaupart, C. Gariépy, L. Z. Cheng, L. Guillou-Frottier, G. Bienfait, and R. Lapointe, Heat flow and deep thermal structure near the southeastern edge of the Canadian Shield, *Can. J. Earth Sci.*, in press, 2000.

Martignole, J., and A. J. Calvert, Crustal-scale shortening and extension across the Grenville province of western Québec, *Tectonics, 15*(2), 376-386, 1996.

McBride, J. H., D. B. Snyder, M. P. Tate, R. W. England, and R. W. Hobbs, Upper mantle reflector structure and origin beneath the Scottish Caledonides, *Tectonics, 14*(5), 1351-1367, 1995.

McHone, J. G., Constraints on the mantle plume model from Mesozoic alkaline intrusions in northeastern North America, *Can. Mineral., 34*, 325-334, 1996.

McHone, J. G., and J. R. Butler, Mesozoic igneous provinces of New England and the opening of the North Atlantic Ocean, *Geol. Soc. Am. Bull., 95*, 757-765, 1984.

Meyer, H. O. A., M. A. Waldman, and B. L. Garwood, Mantle xenoliths from kimberlite near Kirkland Lake, Ontario, *Can. Mineral., 32*, 295-306, 1994.

Morgan, W. J., Convection plumes in the lower mantle, *Nature, 230*, 42-43, 1971.

Morgan, W. J., Deep mantle convection plumes and plate motions, *Am. Assoc. Pet. Geol. Bull., 56*, 203-213, 1972.

Morgan, J. V., M. Hadwin, M. R. Warner, P. J. Barton, and R. P. Ll. Morgan, The polarity of deep seismic reflections from the lithospheric mantle: Evidence for a relict subduction zone, *Tectonophysics, 232*, 319-328, 1994.

Owens, T. J., G. Zandt, and S. R. Taylor, Seismic evidence from an ancient rift beneath the Cumberland Plateau, Tennessee: A detailed analysis of broadband teleseismic *P* waveforms, *J. Geophys. Res., 89*, 7783-7795, 1984.

Percival, J. A., and G. F. West, The Kapuskasing uplift: A geological and geophysical synthesis, *Can. J. Earth Sci., 31*, 1256-1286, 1994.

Pfiffner, O. A., W. Frei, P. Valasek, M. Stäuble, L. Levato, L. DuBois, S. M. Schmid, and S. B. Smithson, Crustal shortening in the Alpine Orogen: Results from deep seismic reflection profiling in the eastern Swiss Alps, line NFP 20-east, *Tectonics, 9*(6), 1327-1355, 1990.

Revenaugh, J., and T. H. Jordan, Mantle layering from *ScS* reverberations, 3, The upper mantle, *J. Geophys. Res., 96*, 19,781-19,810, 1991.

Rivers, T., Lithotectonic elements of the Grenville province: Review and tectonic implications, *Precambrian Res., 86*, 117-154, 1997.

Rivers, T., and D. Corrigan, Convergent margin on southeastern Laurentia during the Mesoproterozoic: Tectonic implications, *Can. J. Earth Sci.*, in press, 2000.

Rivers, T., J. Martignole, C. F. Gower, and A. Davidson, New tectonic divisions of the Grenville province, southeast Canadian Shield, *Tectonics, 8*(1), 63-84, 1989.

Rondenay, S., M. G. Bostock, T. M. Hearn, D. J. White, H. Wu, G. Sénéchal, S. Ji, and M. Mareschal, Teleseismic studies of the lithosphere below the Lithoprobe Abitibi-Grenville Transect, *Can. J. Earth Sci.*, in press, 2000.

Sacks, I. S., The subduction of young lithosphere, *J. Geophys. Res.*, *88*, 3355-3366, 1983.

Saltzer, R. L., and E. D. Humphreys, Upper mantle *P* wave velocity structure of the eastern Snake River Plain and its relationship to geodynamic models of the region, *J. Geophys. Res.*, *102*, 11,829-11,841, 1997.

Sawyer, E. W., and K. Benn, Structure of the high-grade Opatica belt and adjacent low-grade Abitibi Subprovince and Archaean mountain front, *J. Struct. Geol.*, *15*, 1443-1458, 1993.

Sénéchal, G., S. Rondenay, M. Mareschal, J. Guilbert, and G. Poupinet, Seismic and electrical anisotropies in the lithosphere across the Grenville Front, Canada, *Geophys. Res. Lett.*, *23*(17), 2255-2258, 1996.

Silver, P. G., and W. W. Chan, Implications for continental structure and evolution from seismic anisotropy, *Nature*, *335*, 34-39, 1988.

Silver, P. G., and W. W. Chan, Shear wave splitting and subcontinental mantle deformation, *J. Geophys. Res.*, *96*, 16,429-16,454, 1991.

Sleep, N. H., Hotspots and mantle plumes: Some phenomenology, *J. Geophys. Res.*, *95*, 6715-6736, 1990a.

Sleep, N. H., Monteregian hotspot track: A long-lived mantle plume, *J. Geophys. Res.*, *95*, 21,983-21,990, 1990b.

Sleep, N. H., Lateral flow of hot plume material ponded at sublithospheric depths, *J. Geophys. Res.*, *101*, 28,065-28,083, 1996.

Sleep, N. H., Lateral flow and ponding of starting plume material, *J. Geophys. Res.*, *102*, 10,001-10,012, 1997.

Sobolev, S. V., H. Zeyen, G. Stoll, F. Werling, R. Altherr, and K. Fuchs, Upper mantle temperatures from teleseismic tomography of French Massif Central including effects of composition, mineral reactions, anharmonicity, anelasticity and partial melt, *Earth Planet. Sci. Lett.*, *139*, 147-163, 1996.

Sykes, L. R., Intraplate seismicity, reactivation of preexisting zones of weakness, alkaline magmatism, and other tectonism postdating continental fragmentation, *Rev. Geophys.*, *16*(4), 621-688, 1978.

VanDecar, J. C., Upper-mantle structure of the Cascadia subduction zone from non-linear teleseismic travel-time inversion, Ph.D. thesis, 165 pp., Univ. of Wash., Seattle, June 1991.

Van der Lee, S., and G. Nolet, The upper mantle *S* velocity structure of North America, *J. Geophys. Res.*, *102*, 22,815-22,838, 1997.

Vinnik, L. P., Detection of waves converted from *P* to *SV* in the mantle, *Phys. Earth Planet. Inter.*, *15*, 39-45, 1977.

Vinnik, L. P., G. L. Kosarev, and L. I. Makeyeva, Azimuthal anisotropy of the Earth's interior from observations of long-period body waves, *Izv. Earth Phy.*, Engl. Transl., *22*(11), 955-960, 1986.

Warner, M., J. Morgan, P. Barton, P. Morgan, C. Price, and K. Jones, Seismic reflections from the mantle represent relict subduction zones within the continental lithosphere, *Geology*, *24*, 39-42, 1996.

Wessel, P., and W. H. F. Smith, New version of the Generic Mapping Tools released, *Eos Trans. AGU*, *76*, 329, 1995.

White, D. J., D. A. Forsyth, I. Asudeh, S. D. Carr, H. Wu, and R. M. Easton, A seismic-based cross-section of the Grenville Orogen in Ontario and western Quebec, *Can. J. Earth Sci.*, in press, 2000.

White, R., and D. McKenzie, Magmatism at rift zones: The generation of volcanic continental margins and flood basalts, *J. Geophys. Res.*, *94*, 7685-7729, 1989.

Winardhi, S., and R. F. Mereu, Crustal velocity structure of the Superior and Grenville Provinces of the southeastern Canadian Shield, *Can. J. Earth Sci.*, *34*, 1167-1184, 1997.

Wolfe, C. J., and P. G. Silver, Seismic anisotropy of oceanic upper mantle: Shear wave splitting methodologies and observations, *J. Geophys. Res.*, *103*, 749-771, 1998.

Zoback, M. L., Stress field constraints on intraplate seismicity in eastern North America, *J. Geophys. Res.*, *97*, 11,761-11,782, 1992.

M. G. Bostock, R. M. Ellis, and S. Rondenay, Department of Earth and Ocean Sciences, 2219 Main Mall University of British Columbia, Vancouver, British Columbia, Canada V6T 1Z4. (bostock@geop.ubc.ca; ellis@eos.ubc.ca; rondenay@geop.ubc.ca)

T. M. Hearn, Physics Department, New Mexico State University, Box 30001, Dept 3D, Las Cruces, NM 88003-0001. (thearn@atlas.nmsu.edu)

D. J. White, Geological Survey of Canada, 615 Booth Street, Ottawa, Ontario, Canada K1A 0E9. (white@cg.NRCan.gc.ca)

(Received June 11, 1999; revised November 23, 1999; accepted January 25, 2000.)